Accuracy of electromagnetic tracking with a prototype field generator in an interventional OR setting

Lars Eirik Bø[1,2], Håkon Olav Leira[2,3], Geir Arne Tangen[1], Erlend Fagertun Hofstad[1], Tore Amundsen[2,3], and Thomas Langø[1]

[1]SINTEF Technology and Society, Trondheim, Norway
[2]Norwegian University of Science and Technology (NTNU), Trondheim, Norway
[3]St. Olavs Hospital, Trondheim, Norway

November 15, 2011

Abstract

We have studied the accuracy and robustness of a prototype electromagnetic window field generator WFG in an interventional radiology suite with a robotic C-arm. The overall purpose is the development of guidance systems combining real-time imaging with tracking of flexible instruments for bronchoscopy, laparoscopic ultrasound, endoluminal surgery, endovascular therapy and spinal surgery.

The WFG has a torus shape, which facilitates X-ray imaging through its centre. We compared the performance of the WFG to that of a standard field generator SFG under the influence of the C-arm. Both accuracy and robustness measurements were performed with the C-arm in different positions and poses.

The system was deemed robust for both field generators, but the accuracy was notably influenced as the C-arm was moved into the electromagnetic field. The SFG provided a smaller root-mean-square position error, but was more influenced by the C-arm than the WFG. The WFG also produced smaller maximum and variance of the error.

EM tracking with the new WFG during C-arm based fluoroscopy guidance seems to be a step forward, and with a correction scheme implemented it should be feasible.

Medical Physics, vol. 39, no. 1, pp. 399–406, 2012

1 Introduction

Electromagnetic-based navigation of flexible instruments has been explored in various applications. The advantage of this technology is that it does not require a clear line of sight, thus permitting the tracking of instruments in confined spaces and inside the body. This is especially useful for flexible instruments such as catheters, endoscopes and endoscopic ultrasound probes. In endovascular therapy, tracking of guide wires, catheters and needles has been tested, especially for treatment of abdominal aortic aneurisms. Here, tracking has been used to guide e.g. deployment of stent grafts.[1, 11] Similar technology has been applied to cardiac interventions, most notably to catheter-based ablation therapies for treatment of atrial fibrillation.[15] In pulmonology, electromagnetic-based navigated bronchoscopy based on preoperative CT imaging has been introduced, particularly for the diagnosis and targeting (biopsy) of small, peripheral lesions. This has shown to increase the success rate from as low as 30 % to about 67 %.[4, 10] In laparoscopic surgery, electromagnetic (EM) tracking has been proposed, especially to guide flexible laparoscopic ultrasound probes and ablation probes in liver surgery.[6, 13] Preliminary tests combining small ultrasound probes and navigation for spinal surgery also indicate that the added flexibility provided by EM tracking may be advantageous. In addition, several commercial products exist, such as StealthStation Axiem (Medtronic Navigation, Louisville, USA), PercuNav (Philips Healthcare, DA Best, The Netherlands), iGuide CAPPA (Siemens AG, Munich, Germany), i-Logic (SuperDimension Gmbh, Dusseldorf, Germany) and ig4 (Veran Medical Technologies, Inc., St. Louis, USA).

In a setup using EM tracking, the placement of the field generator, which is responsible for generating the EM measurement volume, could influence the setup of other equipment and potentially restrict the movement of the medical personnel. It may also influence how imaging can be performed, e.g. by obstructing X-rays at certain angles. Northern Digital Inc. (NDI) has designed a new prototype field generator, referred to as a window field generator, in an attempt to bypass some of these limitations. This field generator has a torus shape, and the central opening facilitates X-ray imaging with the field generator mounted directly underneath the operating table. This way, the field generator is out of the way and may stay in place throughout the procedure, even when X-ray imaging is required.

EM tracking is vulnerable to disturbances from ferromagnetic interference sources in the surroundings, which may influence the accuracy of the system. It is therefore important to assess the accuracy, not only for each system, but also for each new location where the system is to be used. If there are disturbances that are constant and may be properly characterized, they may be compensated using static correction schemes.[3, 8, 12] However, since the interference depends on the surroundings, it must be char-

acterized for each new location and the correction scheme must be adapted accordingly. Also, if the environment changes during the procedure, e.g. by introduction of additional equipment, this must be taken into account.

Wilson et al. [14] have presented a protocol for accuracy evaluation of EM tracking and applied it to various operating room (OR) settings. A similar protocol was adapted by Yaniv et al. [17] in their overall assessment of EM tracking in the clinical environment. The two works report root-mean-square (RMS) errors in the range of 0.79 mm to 6.67 mm and 0.38 mm to 6.49 mm respectively for various combinations of tracking systems and OR environments. Yaniv et al. have also considered the robustness of the various systems. The robustness is a measure of the resistance to distortion upon introduction of additional equipment to the work volume. If the system is robust, this means that any disturbance is constant and fixed relative to the EM transmitter. This makes it possible to apply a static correction scheme.

In this article, we have adapted the protocol described by Yaniv et al. to study the accuracy and robustness of an EM tracking system within the setting of a new interventional radiology suite. The goal was to compare the performance of the new prototype field generator with that of the original field generator, and to study the influence of a new C-arm on the tracking system.

2 Materials and methods

2.1 Experimental Setup

Our study was done in one of the new interventional radiology suites at St. Olavs University Hospital in Trondheim. The suite, which was opened in august 2010, is a part of the project The Operating Room of the Future (see http://www.stolav.no/for) and is used for both research projects and routine clinical procedures within interventional radiology. The OR is equipped with a robotically controlled cone beam CT imaging system (Siemens Artis zeego, Siemens Healthcare, Forchheim, Germany) referred to as a C-arm.

For position tracking, we used the Aurora Electromagnetic Measurement System (NDI, Waterloo, Canada). The system consists of the utility software NDI ToolBox, a system control unit, four system interface units for position sensor inputs and a field generator that generates an EM tracking volume. This is shown in Fig. 1. In our setup, we used two different field generators: the standard, commercially available, rectangular field generator (SFG) and the prototype window field generator (WFG). The SFG operates with either a cube-shaped measurement volume with side lengths 0.5 m or an extended, dome-shaped volume with side lengths up to 0.96 m. In this study, we used the cube shaped measurement volume. The WFG operates

only with a reduced, dome-shaped measurement volume with side lengths up to 0.65 m.

The main feature of the new prototype is its torus shape, which allows for X-ray images to be taken through the centre opening. However, since the C-arm potentially is a major source of EM interference, the common practice for EM-based navigated procedures has been to remove the C-arm unit from the operating field during navigation. But to a clinician such an approach is cumbersome, as it would be preferable to do imaging and navigation concurrently, or at least intermittently. In an operating room, there are many people, trolleys with equipment, wires and tubes, so that moving the large fluoroscopy unit back and forth is unpractical and time-consuming. In order to take full advantage of the new field generator, it would therefore be advantageous to be able to perform tracking with the C-arm in or close to the operating field. We have therefore analyzed the accuracy and robustness of the tracking in this setting.

All data acquisition was performed using the NDI ToolBox. Four tools with position sensors were used, each having either five or six spatial degrees of freedom (DOF): a Traxtal Reference Tool with six DOF, a custom-designed catheter tool containing an Aurora Micro 6DOF Sensor, an Aurora Tracking Needle with five DOF and an Aurora 6DOF Cable Tool. The tools are shown in Fig. 1 (b). The catheter tool was made from an ordinary, one-lumen catheter with diameter 1.7 mm. The Aurora sensor was inserted into the lumen and fixed with epoxy glue near the tip of the catheter. A pivot calibration procedure was performed using the NDI ToolBox software during tool characterization to determine the position of the tip of the catheter relative to the embedded sensor.

The field generator was mounted underneath the operating table giving no restrictions to the movement of the robotically controlled C-arm. We used the same accuracy phantom as Yaniv et al. [17]: a Plexiglas cube with sides measuring 180 mm and with 225 parallel holes precisely machined from one side, each with diameter 1.9 mm and depth in the range of 10 mm to 150 mm. The phantom was equipped with a reference tool and placed on the operating table approximately in the centre of the tracking system's measurement volume as shown in Fig. 2. In this way, our experimental setup represented a navigation volume relevant for a clinical setup. This setup was used throughout all of the following experiments.

2.2 Tracking System Accuracy Analysis

The catheter tool was manually inserted into each of the 225 holes in the phantom, all the way to the bottom, and 100 position samples were collected from each hole. Since the diameter of the catheter was only 0.2 mm less than the diameter of the hole, this provided an accurate measurement of the position of the bottom of the hole. The procedure was performed

(a)

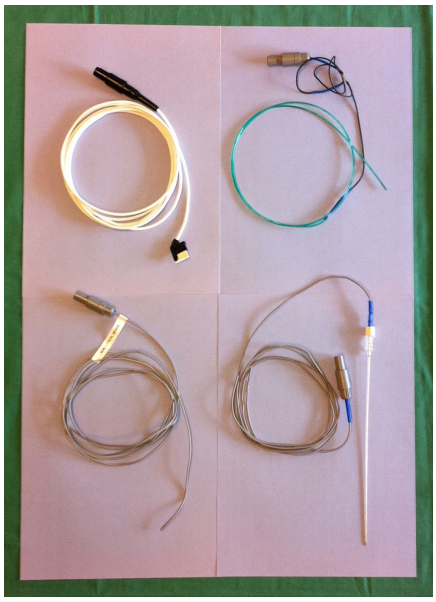

(b)

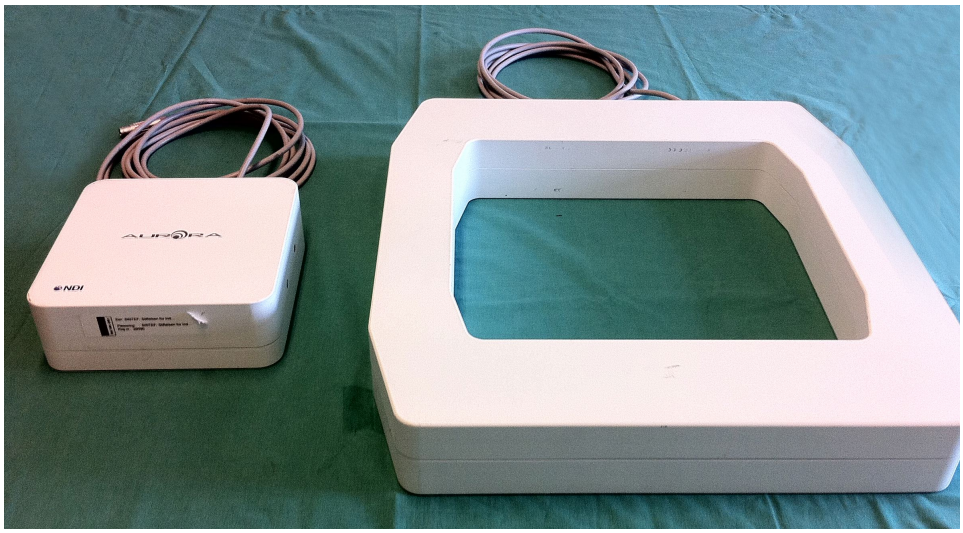

(c)

Figure 1

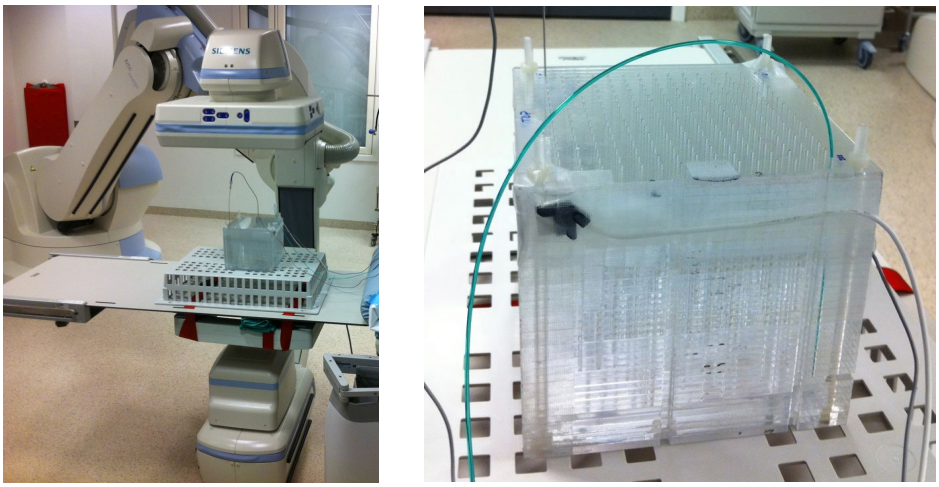

(a) (b)

Figure 2: The accuracy phantom and its setup. The field generators were mounted directly underneath the operating table (the photo shows the WFG). The phantom was equipped with the Traxtal Reference Tool, here seen in the front left corner, and placed on the operating table approximately in the centre of the tracking system's measurement volume. The catheter tool used for the accuracy measurements is seen inserted into the hole in the front right corner of the phantom. For the robustness measurements, two more tools were used: the Aurora Tracking Needle was inserted into the hole in the rear left corner of the phantom and the Aurora 6DOF Cable Tool was attached to the rear right corner.

first with the C-arm inside the tracking system's measurement volume, and then repeated with the C-arm outside the measurement volume. These two measurement experiments were done for both the SFG and the WFG.

For data processing, we used a modified version of a MATLAB software application implemented by Wilson et al. [14]. For each of the 225 holes, a representative transformation was calculated from the 100 recorded position samples. The translational part of this transform was estimated as the arithmetic mean of the acquired translation data, and the rotational part as the arithmetic mean of the acquired rotation data, given in unit quaternions, followed by normalization. In addition, the distance from the origin of the tracking system to each of the 100 position samples was calculated, and the sample variability for the given hole, defined as the difference between the largest and the smallest of these distances, was found. The sample variability is a simple measure of the precision of the performed measurements.

A paired-point rigid registration [7] was then performed between the tracking system and the phantom coordinate system using 9 of the 225 sampled positions. For each of the 225 holes, the distance between the known point coordinate and the estimated representative transformation, transformed by the registration matrix, was calculated. Also, the angular difference between the known orientation of the hole and the measured orientation of the catheter tool was found. The MATLAB application provided the following descriptive statistics: maximal sample variability, RMS error, mean error, standard deviation, error range, maximum error and 95th percentile.

2.3 Tracking System Robustness Analysis

The robustness of an EM tracking system was defined by Yaniv et al. as the system's "resilience to distortions arising from tools and imaging apparatus that are introduced and removed from the work volume during the procedure"[17]. This can be equipment containing ferromagnetic metal or emitting EM fields. We have focused our work on the influence of the C-arm on the tracking system accuracy since this is the potentially biggest source of EM disturbance that can be introduced into the measurement volume of the tracking system.

In image-guided interventions, it is common to use a patient-mounted reference tool and track all other tools relative to this. Motivated by this practice, Yaniv et al. quantified the robustness by considering the distance between two stationary tracking sensors for a certain period of time. If the variability of the measured distance is low, it means that the system reports the position of one sensor relative to the other in a consistent manner, and the system is then regarded as robust. This does not guarantee that the reported position is correct, i.e. that the system is accurate, but it means that potential inaccuracies may be corrected using static correction schemes.

The measurements were done with the imaging apparatus both in home position away from the operating field, and in imaging position during both x-ray fluoroscopy imaging and cone beam CT imaging.

We extended the analysis of Yaniv et al. by also including measurements with the C-arm in a number of intermediate positions and different poses and considering not only the variability of the distance measurements in each position, but also how the measurements change between different positions. If the variability is low in each position, but the measurements change from one position to another, this means that the system is robust and a static correction scheme adapted to the given C-arm position can be applied. We also used four tracking sensors rather than just two in order to account for the possibility of anisotropic disturbances; in this way, distortions that are perpendicular to the axis between two of the sensors will influence the measured distance between two of the other sensors.

The Plexiglas phantom and the tracking system were both set up as for the accuracy analysis. The phantom here only served to ensure that the measurements were carried out within the same navigation volume that was used for the accuracy analyses. Inside and on the phantom we placed the three tracked tools in addition to the reference tool. As seen in Fig. 2(b), we tried to distribute the tool positions as much as possible both in the horizontal plane direction and in depth so that the distance between the sensors ranged from 160 mm to 230 mm. The C-arm was then moved stepwise relative to the operating table in various manners as illustrated in Figs. 4(a), (d), (g) and (j): the C-arm was translated along and perpendicular to the table, it was rotated around the table and the X-ray detector was lowered towards the table. For each step, position data for all four tools were recorded for a period of 30 s and stored. With the C-arm in imaging position, we also recorded position data during both x-ray fluoroscopy imaging and cone beam CT imaging. The distances from the reference tool to each of the other three tools were then calculated. This procedure was repeated for both field generators.

3 Results

3.1 Tracking System Accuracy

Statistical measurements of the position and angle error of the catheter tool from the four experiments are summarized in Table 1. A comparison of the results from the SFG and the WFG, without the influence of the C-arm, demonstrates only minor differences. The SFG appears to provide a smaller RMS position error, while the WFG has less maximum and variance of the error. Also note that the maximal variability within the 100 samples of each phantom node is higher for the SFG.

The accuracy measurements show the strong disturbance caused by the

Table 1: Results of the accuracy measurements performed in the radiology suite. The values in the table are in millimeters and degrees.

		C-arm out of field		C-arm in field	
		Pos.	Angle	Pos.	Angle
WFG	Max. sample variability	0.37		0.40	
	RMS error	1.16	1.11	5.09	4.06
	Mean error	1.11	0.63	4.91	3.66
	Standard deviation	0.38	0.73	1.63	1.69
	Error range	1.75	3.41	7.37	7.48
	Maximum error	1.87	3.42	8.47	7.81
	95th percentile	1.69	2.96	7.50	6.53
SFG	Max. sample variability	0.67		1.09	
	RMS error	0.79	1.57	7.59	9.57
	Mean error	0.56	1.00	4.89	9.91
	Standard deviation	0.42	0.91	4.62	2.72
	Error range	2.55	4.82	40.07	15.42
	Maximum error	2.60	4.90	41.35	16.14
	95th percentile	1.44	3.26	14.15	12.72

C-arm on the EM tracking system. The influence is greater when using the SFG, increasing the RMS position error with about 7 mm, compared to 4 mm increase for the WFG. The results when using the SFG have a larger spread of the error as well. And, when performing the measurements, the Aurora system with the SFG was not able to track the catheter tool in three of the 225 phantom nodes, which thus had to be left out of the calculations.

The RMS angle error and spread of the angle of the catheter pointer were also increased with the C-arm in the field for both field generators. The WFG outperformed the SFG with respect to RMS angle error and spread of the angle, both with and without the influence of the C-arm.

3.2 Tracking System Robustness

The variability in measured sensor distance over the period of 30 s for which the C-arm was at a fixed position was relatively small: For all sensors and all positions, the standard deviation of the measurements was below 0.06 mm and the range was below 0.3 mm.

The robustness measurements made during image acquisition are shown in Fig. 3. The plots correspond to those presented by Yaniv et al. [17]

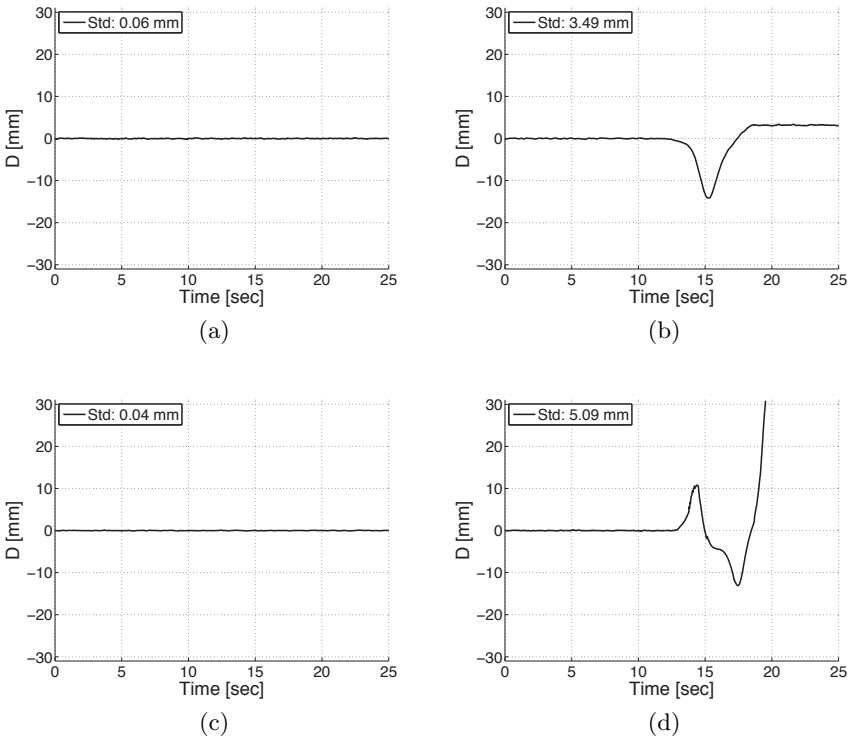

Figure 3: The plots show the variation in measured distance between the Aurora 6DOF Cable Tool and the reference tool during x-ray fluoroscopy imaging (left column) and cone beam CT imaging (right column) measured with the SFG (top row) and WFG (bottom row) respectively.The distance between the sensors is demeaned using the mean of the first 2 s.

and show the distance between the Aurora 6DOF Cable Tool and the reference tool demeaned using the mean of the first 2 s. The imaging sequences were started 10 s after the position measurements, and each sequence lasted approximately 10 s. The measurements show that both field generators are robust to x-ray fluoroscopy imaging, while they are severely influenced by the cone beam CT imaging. The latter caused a deviation of 14.2 mm for the SFG, while the WFG reached a deviation of 30.9 mm before tracking eventually was completely disrupted.

While the tracking system was shown to be robust, except for during cone beam CT imaging, the measured distances between the sensors were strongly affected by the position of the C-arm. In Figs. 4(b), (c), (e) and (f), the mean measured distance from the reference tool to each of the three other tools is plotted as a function of the C-arm's displacement along and perpendicular to the operating table. The distances have been demeaned with the mean of the first recording in each series. This shows that the

difference between the minimum and the maximum measurement as the C-arm is moved along the operating table into the EM field is up to 8 mm for the SFG and 13 mm for the WFG. The same deviation as a function of the C-arm's rotation around the operating table is shown in Figs. 4(h) and (i). Rotation of the C-arm caused a sensor distance alteration of maximum 7 mm. Finally, the effect on the measured sensor distance resulting from moving the X-ray detector closer to the operating table is shown in Figs. 4(k) and (l). Moving the detector 13 cm caused a reduction of the sensor distance of maximum 4 mm.

4 Discussion

When the C-arm was placed far from the measurement volume, the measured accuracy was comparable to that reported by the manufacturer, for both field generators. The results for the SFG are also very close to the values found by Yaniv et al. in a similar interventional radiology suite using the same field generator (see Yaniv et al. [17], Table II, columns 7 and 8). They present a lower maximal sample variability, but slightly higher position errors. The angle errors are almost identical.

When comparing the two field generators, the maximal sample variability was highest for the SFG, which indicates a greater need for smoothing of the measurements, e.g. by averaging a certain number of samples. This kind of noise reduction may, however, reduce the frame rate of the system, or at least introduce a certain time lag, which should be avoided for navigation.

As the C-arm was moved close to the measurement volume and placed directly above the field generator, the EM tracking was strongly influenced, and the measured accuracy went down. The sample variability was relatively unaffected, indicating that the measurements were quite stable, but the measurement error was considerably increased. The SFG performed worse than the WFG: it produced more outliers in the accuracy measurements, with a 95th percentile nearly twice that of the WFG, and it was also unable to track the sensors in certain positions within the measurement volume. The WFG did not present any of these problems, and it thus appears to be more stable. However, with 95th percentile of 7.50 mm and 14.15 mm respectively, the error is considerable in both cases.

The robustness measurements showed that the distances between the various sensors varied little as long as the C-arm stayed in one position: the standard deviation of the measured distance was below 0.06 mm and the range was below 0.3 mm for all positions. This is similar to the results of Yaniv et al., who present a standard deviation of 0.05 mm for Aurora in their interventional radiology suite. The system may thus be said to be robust with respect to the OR and C-arm influence on the EM field. However, the measured distance varied greatly as the C-arm was moved or rotated, which

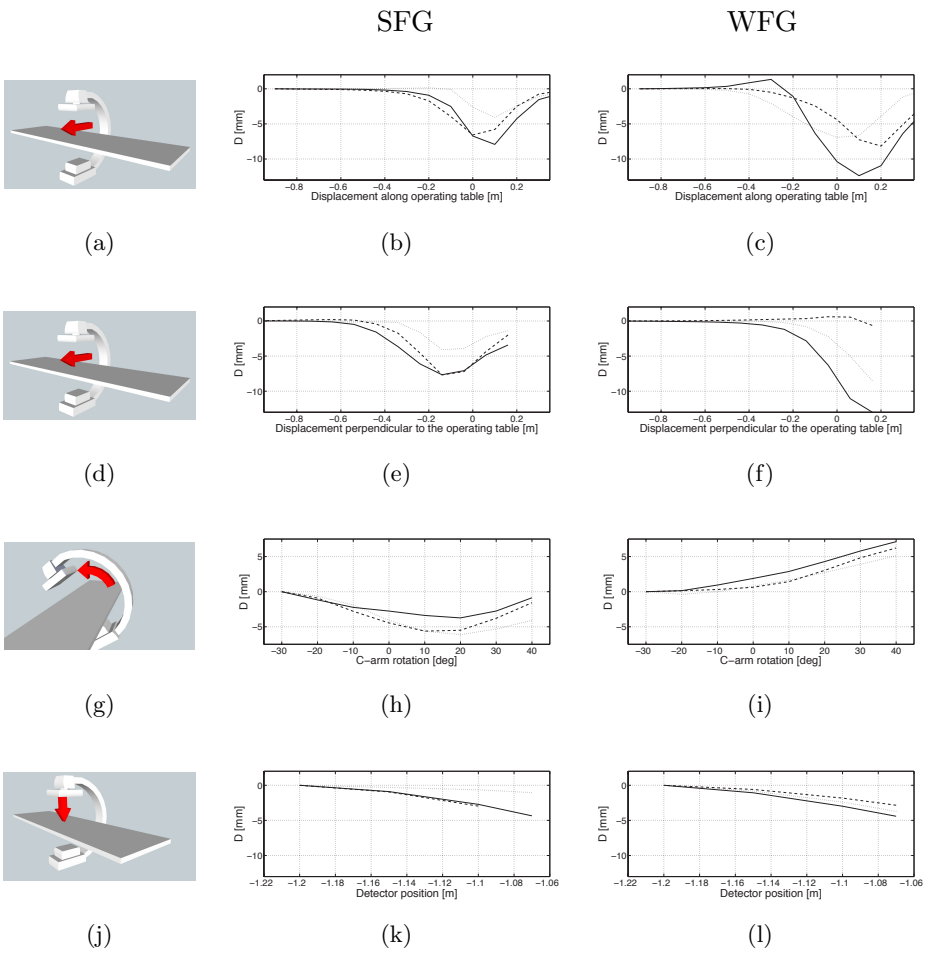

Figure 4: The figures in the left column indicate the stepwise movement of the C-arm relative to the operating table during the robustness measurements. The plots in the middle column show the mean measured distance from the reference tool to each of the three other tools as a function of the C-arm's displacement using the SFG. The plots in the last column show the same results for the WFG. The distances have been demeaned with the mean of the first recording in each series. The actual distances between the tools were between 160 and 230 mm. In the two upper rows, 0 displacement indicates that the C-arm is straight above the measurement volume, and we see that the deviation has a peak close to this point.

is consistent with the poor accuracy that was measured with the C-arm close to the measurement volume. The variation was largest for the WFG, which might be due to the larger measurement volume potentially exposing it to more ferromagnetic interference sources in the surroundings. However, for both field generators the variation was notable, and it is thus clear that a correction scheme is required in order to use the tracking system with the C-arm in this position.

Since the system is robust, a static correction scheme may be adapted. In its simplest form, such a scheme involves measuring the position and orientation of a position sensor at a number of fixed reference points throughout the measurement field. As the C-arm is introduced, the same measurements are repeated. This will provide us with deformation data for the reference points for the given position of the C-arm. Deformations between these reference points can be determined by different interpolation schemes as described by Kindratenko [8]. By mapping the deformation field with this calibration procedure we are then able to correct any further position data readings. This will however only be valid for the given system setup and C-arm position, meaning that a precalibration process must be performed for all relevant C-arm positions. An improved solution could be to place several position sensors throughout the measurement field forming a set of reference points. Distortions detected by these sensors as the C-arm is moved closer and into the measurement field could be used to characterize the deformation field. This opens the possibility of doing calibration and correction of position data in real time.

Hybrid solutions have been investigated, using a combination of optical and electromagnetic tracking. The optical tracking data are not influenced by metal objects in the environment and can be used as reference points.[3, 12] With this technique we may be able to map the deformation field by performing an intraoperative calibration sequence, moving the hybrid tool through the volume of interest before starting navigation.

Other solutions suggested in the literature include merging position data generated from live fluoroscopy images with electromagnetic position tracking data and in this way increase accuracy.[2] Recent work has also shown how statistical models for the tool movement can be used to estimate the tool position.[16, 9, 5] In our future work, we will look into and experiment with these techniques to improve the accuracy and performance of navigation in the clinical environment.

5 Conclusion

EM tracking with the new WFG during C-arm based fluoroscopy guidance seems to be a step forward, and with a correction scheme implemented it should be feasible. With navigation technology, these procedures may be

performed with less imaging, i.e. less X-ray exposure in total. We believe that such a system could be valuable for numerous clinical applications, such as endovascular therapy and navigated bronchoscopy, but also for experimental surgery in e.g. laparoscopy, where the C-arm is used for verification and comparison purposes, and spinal surgery. We will continue to develop EM based tracking integrated in minimal access therapy applications and follow up this study with clinical experiments to demonstrate the potential value in combination with a C-arm.

Acknowledgements

We would very much like to thank Emmanuel Wilson at the Georgetown University Medical Center for providing us with the phantom and MATLAB code used in this work.

This study was supported by: SINTEF (Trondheim, Norway), The Ministry of Health and Social Affairs of Norway, through the National Centre for 3D Ultrasound in Surgery (Trondheim, Norway), project 196726/V50 eMIT (Enhanced minimally invasive therapy, FRIMED program), and the Operating Room of the Future project at St. Olavs Hospital (Trondheim, Norway).

References

[1] N. Abi-Jaoudeh, N. Glossop, M. Dake, W. F. Pritchard, A. Chiesa, M. R. Dreher, T. Tang, J. W. Karanian, and B. J. Wood. Electromagnetic Navigation for Thoracic Aortic Stent-graft Deployment: A Pilot Study in Swine. *Journal of Vascular and Interventional Radiology*, 21 (6):888–895, 2010.

[2] M. Azizian and R. Patel. Data fusion for catheter tracking using Kalman filtering: applications in robot-assisted catheter insertion. In K. H. Wong and D. R. H. III, editors, *Medical Imaging 2011: Visualization, Image-Guided Procedures, and Modeling*, volume 7964, page 796413. SPIE, 2011.

[3] A. J. Chung, P. J. Edwards, F. Deligianni, and G.-Z. Yang. Freehand Cocalibration of Optical and Electromagnetic Trackers for Navigated Bronchoscopy. In G.-Z. Yang and T. Jiang, editors, *Medical Imaging and Augmented Reality*, volume 3150 of *Lecture Notes in Computer Science*, page 320–328. Springer Berlin/Heidelberg, 2004.

[4] R. Eberhardt, D. Anantham, F. Herth, D. Feller-Kopman, and A. Ernst. Electromagnetic Navigation Diagnostic Bronchoscopy in Peripheral Lung Lesions. *Chest*, 131(6):1800 – 1805, 2007.

[5] M. Feuerstein, T. Reichl, J. Vogel, J. Traub, and N. Navab. Magneto-Optical Tracking of Flexible Laparoscopic Ultrasound: Model-Based Online Detection and Correction of Magnetic Tracking Errors. *IEEE Transactions on Medical Imaging*, 28(6):951–967, 2009.

[6] P. Hildebrand, M. Kleemann, S. Schlichting, A. Besirevic, U. Roblick, C. Bürk, and H.-P. Bruch. Prototype of an Online Navigation System for Laparoscopic Radiofrequency Ablation of Liver Tumors. In O. Dössel and W. C. Schlegel, editors, *World Congress on Medical Physics and Biomedical Engineering*, volume 25/6 of *IFMBE Proceedings*, page 352–354. Springer Berlin Heidelberg, 2009.

[7] B. K. P. Horn. Closed-form solution of absolute orientation using unit quaternions. *Journal of the Optical Society of America A*, 4(4):629–642, 1987.

[8] V. Kindratenko. A Survey of Electromagnetic Position Tracker Calibration Techniques. *Virtual Reality*, 5(3):169–182, 2000.

[9] X. Luo, T. Kitasaka, and K. Mori. Bronchoscopy Navigation beyond Electromagnetic Tracking Systems: A Novel Bronchoscope Tracking Prototype. In G. Fichtinger, A. Martel, and T. Peters, editors, *Medical Image Computing and Computer-Assisted Intervention — MICCAI 2011*, volume 6891 of *Lecture Notes in Computer Science*, page 194–202. Springer Berlin/Heidelberg, 2011.

[10] D. Makris, A. Scherpereel, S. Leroy, B. Bouchindhomme, J.-B. Faivre, J. Remy, P. Ramon, and C.-H. Marquette. Electromagnetic Navigation Diagnostic Bronchoscopy for Small Peripheral Lung Lesions. *The European Respiratory Journal*, 29(6):1187–1192, 2007.

[11] F. Manstad-Hulaas, S. Ommedal, G. A. Tangen, P. Aadahl, and T. A. N. Hernes. Side-Branched AAA Stent Graft Insertion Using Navigation Technology: A Phantom Study. *European Surgical Research*, 39 (6):364–371, 2007.

[12] M. Nakamoto, K. Nakada, Y. Sato, K. Konishi, M. Hashizume, and S. Tamura. Intraoperative Magnetic Tracker Calibration Using a Magneto-Optic Hybrid Tracker for 3-D Ultrasound-Based Navigation in Laparoscopic Surgery. *IEEE Transactions on Medical Imaging*, 27 (2):255–270, 2008.

[13] O. V. Solberg, T. Langø, G. A. Tangen, R. Mårvik, B. Ystgaard, A. Rethy, and T. A. N. Hernes. Navigated Ultrasound in Laparoscopic Surgery. *Minimally Invasive Therapy & Allied Technologies*, 18 (1):36–53, 2009.

[14] E. Wilson, Z. Yaniv, H. Zhang, C. Nafis, E. Shen, G. Shechter, A. D. Wiles, T. Peters, D. Lindisch, and K. Cleary. A Hardware and Software Protocol for the Evaluation of Electromagnetic Tracker Accuracy in the Clinical Environment: a Multi-Center Study. In R. C. Kevin and I. M. Michael, editors, *Medical Imaging 2007: Visualization and Image-Guided Procedures*, volume 6509 of *Proceedings of SPIE*, page 65092T. SPIE, 2007.

[15] K. Wilson, G. Guiraudon, D. L. Jones, and T. M. Peters. Mapping of Cardiac Electrophysiology Onto a Dynamic Patient-Specific Heart Model. *IEEE Transactions on Medical Imaging*, 28(12):1870–1880, 2009.

[16] R. Wolf, J. Duchateau, P. Cinquin, and S. Voros. 3D Tracking of Laparoscopic Instruments Using Statistical and Geometric Modeling. In G. Fichtinger, A. Martel, and T. Peters, editors, *Medical Image Computing and Computer-Assisted Intervention — MICCAI 2011*, volume 6891 of *Lecture Notes in Computer Science*, page 203–210. Springer Berlin/Heidelberg, 2011.

[17] Z. Yaniv, E. Wilson, D. Lindisch, and K. Cleary. Electromagnetic Tracking in the Clinical Environment. *Medical Physics*, 36(3):876–892, 2009.